

## *Supporting Information*

# **Organogel Assisted Porous Organic Polymer Embedding Cu Nanoparticles for Selectivity Control Semi Hydrogenation of Alkynes**

Ratul Paul,<sup>a,b,h</sup> Subhash Chandra Shit,<sup>a,b,h</sup> Arunima Singh,<sup>c,h</sup> Roong Jien Wong,<sup>d</sup> Duy Quang Dao,<sup>e,f</sup> Bobby Joseph,<sup>g</sup> Wen Liu,<sup>\*,d</sup> Saswata Bhattacharya<sup>\*,c</sup> and John Mondal<sup>\*,a,b</sup>

<sup>a</sup>Catalysis & Fine Chemicals Division, CSIR-Indian Institute of Chemical Technology, Uppal Road, Hyderabad 500 007, India. E-mail: [johncuchem@gmail.com](mailto:johncuchem@gmail.com); [johnmondal@iiict.res.in](mailto:johnmondal@iiict.res.in) (J.M.)

<sup>b</sup>Academy of Scientific and Innovative Research (AcSIR), Ghaziabad-201002, India.

<sup>c</sup>Department of Physics, Indian Institute of Technology Delhi Hauz Khas, New Delhi 110 016, India. E-mail: [saswata@physics.iitd.ac.in](mailto:saswata@physics.iitd.ac.in) (S.B.)

<sup>d</sup>School of Chemical and Biomedical Engineering, Nanyang Technological University, 62 Nanyang Avenue, Singapore 637459. E-mail: [wenliu@ntu.edu.sg](mailto:wenliu@ntu.edu.sg) (W.L.)

<sup>e</sup>Institute of research and development, Duy Tan University, Da Nang, 550000, Viet Nam.

<sup>f</sup> Faculty of Environmental and Chemical Engineering, Duy Tan University, 550000, Da Nang, Viet Nam.

<sup>g</sup>Elettra-Sincrotrone Trieste, S.S. 14, Km 163.5 in Area Science Park, Basovizza 34149, Italy

<sup>h</sup>All the three authors have equally contributed in the manuscript.

## Table of Contents

Characterization Technique Details.....	S3
Computational details.....	S5
Experimental section.....	S6
N <sub>2</sub> -adsorption/desorption isotherms.....	S11
Pore-size distribution.....	S12
Thermo gravimetric analysis (TGA).....	S13
Table of HOMO, LUMO energies and band gaps.....	S14
Table for Cartesians coordinates of keto-form based polymer and two precursors calculated at the B3LYP/6-31+g(d,p) level of theory in the gas phase .....	S15
<sup>13</sup> C Cross Polarization (CP) solid state MAS NMR spectra.....	S20
TEM images of POP.....	S21
FE-SEM images.....	S22
Energy dispersive X-ray (EDX) spectroscopy.....	S24
Wide angle powder X-ray diffraction patterns.....	S25
Particle size distribution histogram profile.....	S26
X-ray photoelectron spectra (XPS).....	S27
Solvent effect.....	S29
Recyclability test.....	S36
Reused catalyst characterization.....	S37
Adsorption energies (E <sub>ads</sub> ) calculation.....	S39
Comparison study.....	S41
References.....	S44

### **Characterization Technique Details:**

Powder X-ray diffraction (XRD) patterns of the catalysts were performed on a Rigaku Miniflex (Rigaku Corporation, Japan) X-ray diffractometer using Ni filtered Cu K $\alpha$  radiation ( $\lambda = 1.5406 \text{ \AA}$ ) with a scan speed of  $2^\circ \text{ min}^{-1}$  and a scan range of  $10\text{-}80^\circ$  at 30 kV and 15 mA.

The morphology of the catalysts was obtained by scanning electron microscopy (SEM) technique. The SEM equipment was FEI Verios 460L field-emission SEM (FE-SEM) which is an ultra-high resolution Schottkey emitter SEM equipped with an electron diffraction spectroscopy (EDS) detector. Thus, the elemental mapping EDS analysis were also performed in the same SEM instrument. Transmission electron microscopy (TEM) images of the catalysts were captured at 100 kV on a JEOL 1010 TEM.

The surface area was determined through the Brunauer-Emmett-Teller (BET) method. The average pore volume and pore size were measured by Barrett-Joyner-Halenda (BJH) method. The BET surface area, pore volume and pore sizes were determined by using the N<sub>2</sub> adsorption-desorption method using BEL Sorb II Instruments, Japan at liquid nitrogen temperature. Before the measurement the samples were degassed at 200 °C for 2 h.

X-ray photoelectron spectroscopy (XPS) were investigated on a Thermo Scientific K-Alpha instrument (monochromatic Al K $\alpha$  radiation, E<sub>photon</sub> = 1486.6 eV). The binding energy (B.E) in each case, that is, core levels and valence band maxima were corrected using an internal reference peak of C 1 s peak centered at 284.8 eV.

FT-IR spectrums of catalysts were investigated on a DIGILAB (USA) IR spectrometer using the KBr disc method.

Solid-state <sup>13</sup>C CP MAS NMR studies were performed by using a Bruker Avance III HD 400 MHz NMR spectrometer.

### **Product Analysis by Gas Chromatography (GC/GC-MS):**

All the reactants, products and intermediate are confirmed and analyzed by GC-MS (Model QP 5050 supplied by M/S. Shimadzu Instruments Corporation, Japan) and GC (Shimadzu 2010) respectively. The GC is equipped with flame ionization detector (FID) and INNO Wax capillary column (diameter: 0.25 mm, length: 30 m) is used for the separation of the reaction mixtures. The product and reactant mixture which are collected from the reactor was added into the organic solvents (methanol or acetone) and equal amount of an internal standard (anisole) was added before starting the GC analysis. The GC programming conditions are different for different reactions. The temperature of the injector is 250°C, the temperature of oven/column is usually 80-280 °C with the ramping rate of 10 °C min<sup>-1</sup> and holding time is 3 and 5 minutes for starting and the end time of the analysis respectively. The FID temperature is 300 °C.

The solution was analysed by a HP 5890 series II GC equipped with DB-WAX column (polar, 30 m, 0.32 mm diameter, 0.25 mm film thickness) and mass data were evaluated by Jeol JMS-AX505WA mass spectrometer. 1 ml sample in organic phase was injected (split ratio 1:80) with helium as carrier gas, and the temperature of oven was programmed for efficient separation of peaks (temperature increment of 15 °C/min from 50 °C up to 200 °C). The temperature of injector was 250 °C. Ionizing energy for MS operation was 70 eV.

### **DRIFTS experimental procedure:**

Diffuse reflectance infrared Fourier transform spectroscopy (DRIFTS) was performed with a Bruker Vertex 80 FTIR spectrometer and a Harrick Scientific Praying Mantis diffuse reflection accessory. The catalyst samples were diluted with spectroscopy grade KBr and were loaded into the Praying Mantis high temperature reaction chamber. The samples were preheated to 150°C under constant flow of dry air to remove surface moisture. A drop of styrene was added to the catalyst samples. FTIR spectra were collected continuously for 5min until no further changes were observed. The catalyst samples were then cooled to

room temperature. All measurements were collected with the MCT detector, averaged over 32 scans with 4 cm<sup>-1</sup> resolutions.

### **Computational details:**

All calculations were performed by employing Gaussian 16 Rev.A.03 package<sup>1</sup>. Geometries and electronic structures of gel precursors [A] and [B] were investigated in the gas phase using Becke three-parameter hybrid functionals B3LYP density functional (DFT)<sup>2</sup>. This functional was combined with the basis set 6-31+G(d,p). This approach was recommended by different computational works which approved good accuracy for this type of organic molecular systems<sup>3,4</sup>. Energies of frontier orbitals (i.e., the highest occupied molecular orbital-HOMO, and the lowest unoccupied molecular orbital-LUMO) and their energy gap were also calculated at the same level of theory.

In order to study semi-hydrogenation of phenyl acetylene on Cu@TpRb-POP-A and Cu@TpRb-POP-B, we have employed Density Functional Theory (DFT) for conducting first-principles based calculations. The Vienna *Ab initio* Simulation Package (VASP) based on PAW pseudopotentials and plane wave basis set have been utilized.<sup>5,6</sup> The Generalized Gradient Approximation (GGA) have accounted the interactions of electronic exchange and correlation (xc), with the functional form of Perdew-Burke-Ernzerhof (PBE).<sup>7</sup> The energy tolerance and atomic forces have been converged up to 0.001 meV and 0.001 eV/Å, respectively, with the conjugate gradient minimization. The ground state calculations have been conducted with the plane wave energy cutoff of 500 eV. The van der Waals correction as per the Tkatchenko-Scheffler scheme have been included in the calculation.<sup>8,9</sup> We have calculated the free energy change ( $\Delta G$ ) at each reaction step as per the expression:

$$\Delta G = \Delta E + \Delta E_{\text{ZPE}} - T\Delta S$$

where  $\Delta E$  is the energy obtained from DFT,  $\Delta E_{\text{ZPE}}$  is the zero-point energy and  $\Delta S$  is the entropic contribution.<sup>10</sup>

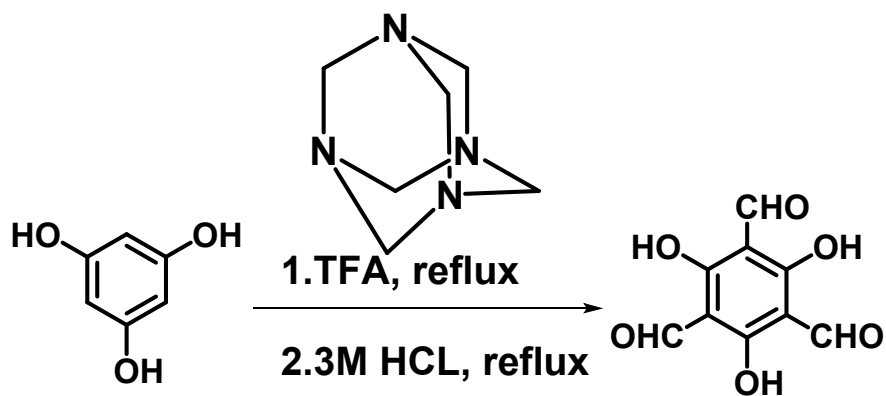
### **Experimental Section:**

## Materials & Methods:

All the chemicals including phloroglucinol, hexamethylenetetramine, trifluoroacetic acid, pararosanine base, acetic acid, copper (II) chloride dihydrate ( $\text{CuCl}_2 \cdot 2\text{H}_2\text{O}$ ), HCl and  $\text{NaBH}_4$  were purchased from Sigma-Aldrich and used as received. All the solvents 1,4-dioxane, dichloromethane, distilled water and was purified and dried before the reaction.

### Synthesis of 1, 3, 5-Triformylphloroglucinol (TFP)

Dried phloroglucinol and Hexamethylenetetramine were mixed in trifluoroacetic acid (TFA) (45 ml) thoroughly in a 250 mL RB and heated at  $80^\circ\text{C}$  for 3 hours under  $\text{N}_2$  atmosphere. After that, 75 ml HCl ( $3 \text{ mol L}^{-1}$ ) was added to the solution and again heated at  $80^\circ\text{C}$  for another 1 hour. Then, the reaction mixture was cooled down to room temperature and filtered through celite bed utilizing dichloromethane (DCM). Finally, the as-obtained organic compound TFP was collected by using a rotary evaporator and dried under vacuum. The as-synthesized organic monomer TFP was confirmed by  $^1\text{H}$  and  $^{13}\text{C}$  NMR technique.<sup>11</sup>



**Scheme S1:** Synthesis procedure of 1, 3, 5-Triformylphloroglucinol (TFP).

### **Synthesis of Pararosaniline based Porous-Organic-Gel-Polymer (TpRb-POP)**

1,3,5-triformylphloroglucinol (TFP) (210 mg, 1 mmol) and pararosaniline base (PAB) (305 mg, 1 mmol) were taken in a 25 mL flat bottom glass vial and 5 mL of 1,4-dioxane solvent was added to the mixture. Then the reaction mixture was sonicated for 2 minute and subsequently, heated at 80°C for 5minute. After that, an aqueous solution of acetic acid (1.0 ml, 3.0 M) was added dropwise to the previous solution and kept the solution for 10minute. After 10 minute the gel was formed which was dried in a vacuum oven at 60°C and leveled as TpRb-POP.

### **Synthesis of Cu@TpRb-POP-A and Cu@TpRb-POP-B**

Typically, 250 mg of TpRb-POP was dispersed in 200 mL of H<sub>2</sub>O *via* sonication for 15 min, followed by the addition of 50 mL aqueous solution of Cu (NO<sub>3</sub>)<sub>2</sub>.3H<sub>2</sub>O (80 mg, 0.3 mmol) and stirred at room temperature for 12 hours. After that a dark brown color product Cu (II)@TpRb-POP was isolated by centrifugation, washed thoroughly with MeOH and dried under vacuum. For Cu@TpRb-POP-A synthesis, ice-cold solution of NaBH<sub>4</sub>(1mmol in 10ml H<sub>2</sub>O) was added dropwise to the well-dispersed solution of Cu (II)@TpRb-POP obtained after the stirring at room temperature for 12 h as described earlier, followed by continuous stirring for 1 hour at room temperature. Finally, Cu@TpRb-POP-A was isolated by centrifugation, thoroughly washed with MeOH and dried overnight under vacuum.

For Cu@TpRb-POP-B synthesis, the as-obtained Cu (II)@TpRb-POP was reduced *via* solid-state reduction technique employing a stream of H<sub>2</sub>/N<sub>2</sub> (10% H<sub>2</sub>, 100 mL min<sup>-1</sup>) at 250°C for 3 h, yielding a dark black solid, leveled as Cu@TpRb-POP-B.

### **Synthesis of Cu-DVAC-1:**

DVAC-1 Porous-Organic-Polymer has been synthesized following the previous literature procedure by Zhao *et al.* In a typical synthesis procedure, divinylbenzene (5.99 mmol, 781 mg) and acrylic acid (1.49 mmol, 108 mg) were mixed together in a round-bottomed flask containing acetone (15 mL). To the mixture, AIBN (0.152 mmol, 25 mg) was added and

the resulted mixture was allowed to stir at room temperature under nitrogen atmosphere for 10 h. Then, the resultant mixture was hydrothermally treated in an autoclave at 120°C under static condition for 24 h. The final white color solid material DVAC-1 was isolated and dried in air. 250 mg of DVAC-1 was dispersed in 200 mL of H<sub>2</sub>O *via* sonication for 15 min, followed by the addition of 50 mL aqueous solution of Cu (NO<sub>3</sub>)<sub>2</sub>·3H<sub>2</sub>O (80 mg, 0.3 mmol) and stirred at room temperature for 12 hours. Then the solid Cu-POP composite was reduced under the stream of H<sub>2</sub>/N<sub>2</sub> (10% H<sub>2</sub>, 100 mL/min) at 250°C for 3 h, yielding a dark brown solid, denoted as Cu-DVAC-1.

#### **Synthesis of Cu-SBA-15:**

For synthesis of pure SBA-15, P123 (2.0 g) was dissolved in aqueous HCl (60 mL, 2.0 M). The mixture was stirred at 25°C with the addition of distilled water (15.0 g). After getting a clear solution, tetraethyl orthosilicate (TEOS, 4.25 g) was added drop-wise to the solution at 25°C. After the complete addition of TEOS, the mixture was stirred at 25°C for 24 h, and then transferred into a Teflon-lined autoclave and kept at 100°C for another 24 h. Finally, the solid product was recovered by filtration, washed with distilled water, and air dried. Calcination step was performed at 500°C in air for 5 h to remove the template, and pure calcined SBA-15 was obtained. After that Cu-SBA-15 composite was reduced with the similar method under stream of H<sub>2</sub>/N<sub>2</sub> (10% H<sub>2</sub>, 100 mL/min) at 250°C for 3 h, to furnish brown solid.

#### **General reaction procedures:**

Phenyl Acetylene (PA) (0.11ml, 1 mmol), catalysts (30 mg), isopropanol (30 mL) were charged into 100 mL stainless steel Parr autoclave inbuilt with a pressure gauge setup. Then, the reactor was evacuated by employing a vacuum pump for 10 min at room temperature to remove dissolved O<sub>2</sub> or air and after that pressurized with H<sub>2</sub> from 0.4 MPa

to 2 MPa. Then according to reaction requirement, we had set the temperature of the autoclave (from 40°C to 150°C) for the desired reaction time with continuous stirring at 400 rpm. After completion of the reaction, the autoclave was cooled to room temperature and catalyst was recovered from the solution by centrifugation. The reaction solutions were examined by a gas chromatograph (Shimadzu 2010) equipped with a flame ionization detector using INNO Wax capillary column (diameter: 0.25 mm; length: 30 m). The products were also checked by gas chromatography-mass spectrometry (Shimadzu, GCMS-QP2010S)

#### **Catalyst Recyclability Test:**

Usually, recyclability of Phenyl Acetylene semihydrogenation with Cu@TpRb-POP-A and Cu@TpRb-POP-B catalysts were carried out taking a mixture of Phenyl Acetylene (1ml, 10 mmol), catalyst (200 mg), and isopropanol (150 mL) in a 200 mL dry stainless-steel reactor and stirred the resulting mixture at 150°C and 20 bar H<sub>2</sub> pressure for 10 h. After finishing the reaction, the catalyst was retrieved from the as-obtained solution through centrifugation and washing with methanol with several times. At last, the catalyst was dried in an oven for 24 h. Then the catalyst was employed for the next cycle reaction.

#### **Hot filtration test:**

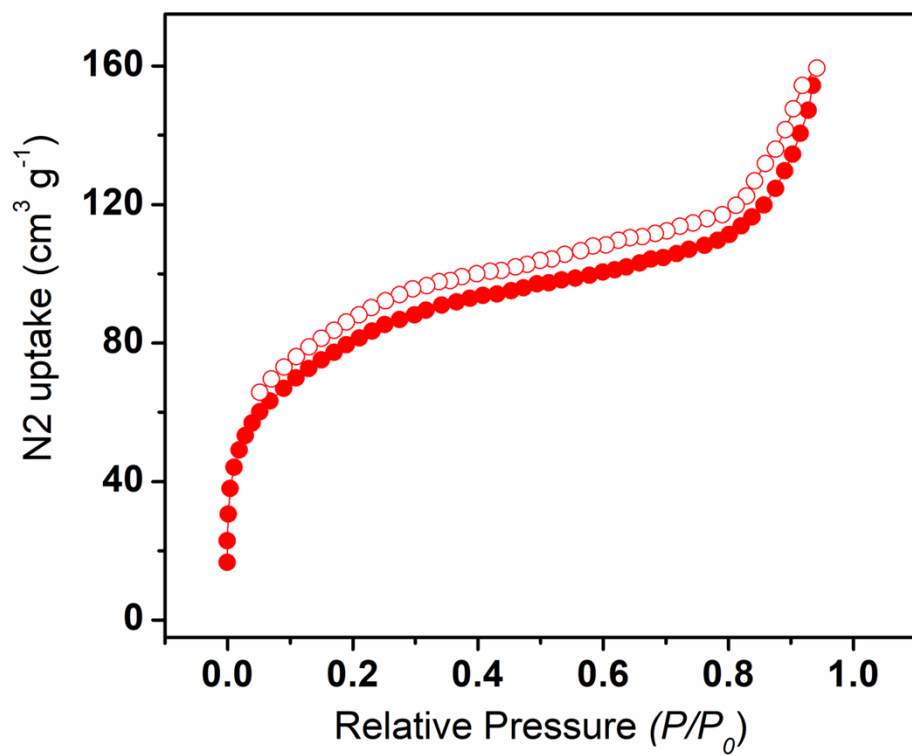
To reveal the robustness and heterogeneity nature of our catalyst we have examined hot filtration test. Normally, a mixture of Phenyl Acetylene (0.11ml, 1mmol), catalyst (30mg), and isopropanol (30 mL) was taken in a 50 mL dry stainless-steel autoclave and stirred the reaction mixture at 150 °C under 20 bar H<sub>2</sub> pressure. After 5 min. the catalyst was separated from the hot reaction mixture and the as-obtained filtrate solution was analyzed through GC technique, which clearly showed 30% Phenyl Acetylene conversion with 27% styrene selectivity in case of Cu@TpRb-POP-A, while Cu@TpRb-POP-B exhibits only 24%

conversion with 22% styrene selectivity. Then under similar reaction condition we have carried out the reaction for 10 h where no obvious increase in Phenyl Acetylene conversion and styrene selectivity were found for both the catalyst, as evidenced by GC analysis. This fact unambiguously proves that the Cu nanoparticles were tightly bound within rigid porous organic polymer framework, making the system heterogeneous in nature.

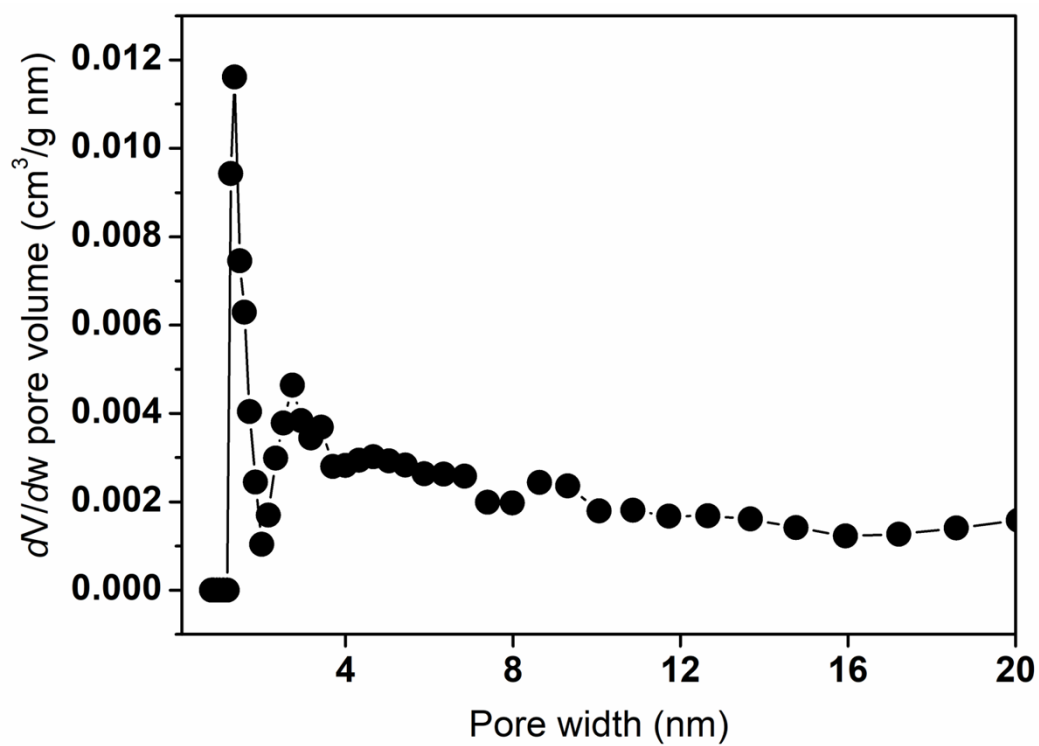
### **TOF calculation**

The initial turn over frequency (TOF) of the catalyst was calculated by this equation.

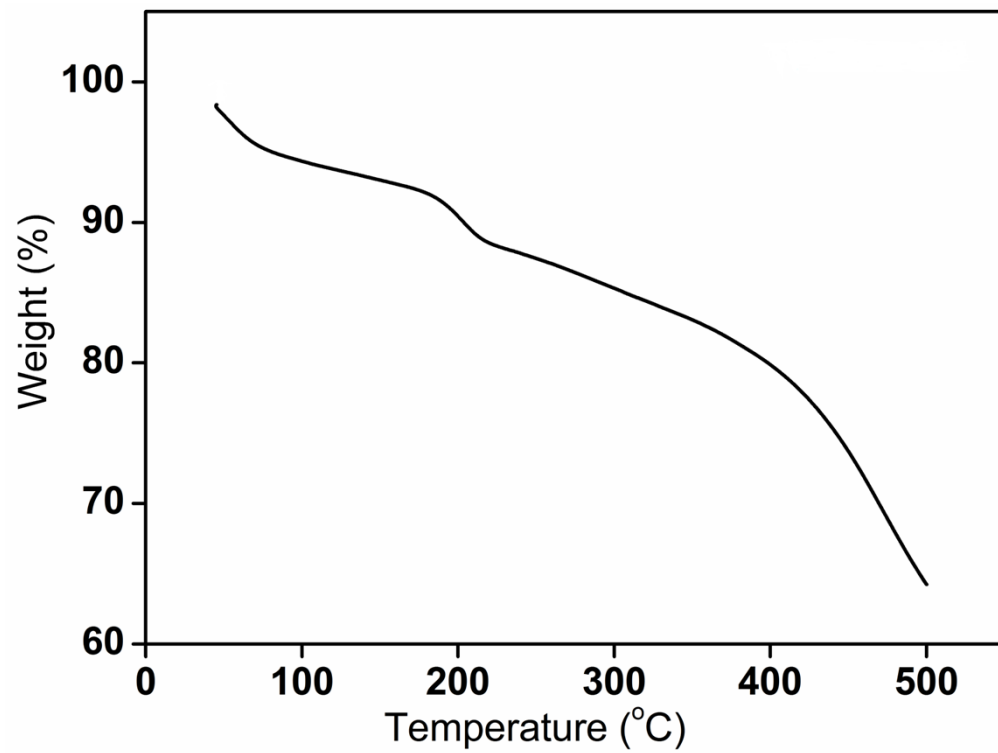
$$\text{TOF} = \frac{(\text{moles of product})}{\{(\text{moles of metal in catalyst}) \times (\text{reaction time})\}}$$



**Figure S1:** N<sub>2</sub>-adsorption/desorption isotherms of TpRb-POP.



**Figure S2:** Pore-size distribution as measured by nonlocal density functional theory modeling (NLDFT) of TpRb-POP.

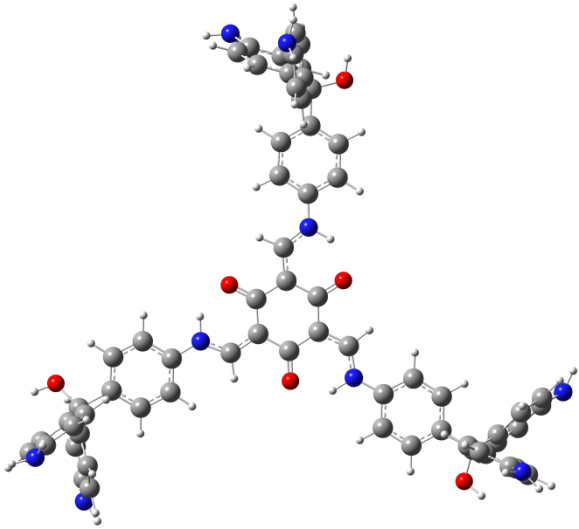


**Figure S3:** Thermogravimetric analysis (TGA) of **TpRb-POP**.

**Table S1:** HOMO, LUMO energies and band gaps (in eV) of two precursors and of the polymer.

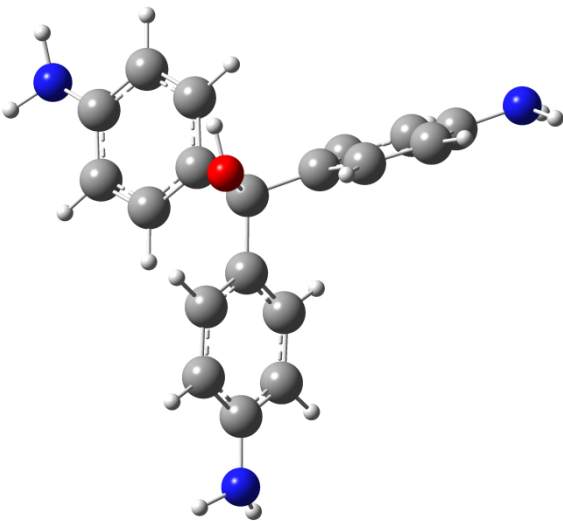
	$E_H$	$E_L$	$DE_{L-H}$
<b>[A]</b>	-0.31	-0.17	0.14
<b>[B]</b>	-0.29	-0.16	0.13
<b>POP</b>	-0.28	-0.19	0.10

**Table S2:** Cartesians coordinates of keto-form based polymer and two precursors calculated at the B3LYP/6-31+g(d,p) level of theory in the gas phase.

	A-3B polymer			Optimized structure
O 1				
C	-1.10346300	0.93871600	-0.20815600	
C	1.36539600	0.48754700	-0.20149600	
C	-0.25985000	-1.42501600	-0.21296300	
C	0.26179900	1.45285000	-0.20000800	
C	-1.38768600	-0.49966600	-0.21309700	
C	1.12788500	-0.95189400	-0.20624500	
C	-2.19811400	1.79367600	-0.21071100	
C	2.65330900	1.00784800	-0.19680400	
H	-3.18203300	1.33623400	-0.21613400	
H	2.74974400	2.08860500	-0.19080600	
O	-2.57408600	-0.92487700	-0.21694400	
O	2.08928500	-1.76682300	-0.20369300	
H	3.56794600	-0.74282000	-0.19649400	
O	0.48660600	2.69291500	-0.19217100	
H	-1.14011400	3.46160400	-0.19744600	
N	3.76623900	0.26820100	-0.19707500	
N	10.19710500	5.85795100	-4.25560400	
N	11.21467400	3.32385900	5.11927700	
C	9.31063500	1.88678900	-0.14737300	
C	7.82953400	1.47103300	-0.18626000	
C	9.58121300	2.96882000	-1.21162500	
C	9.75911900	2.32097300	1.26072200	
C	7.45652800	0.12177000	-0.13353700	
C	9.53552000	4.34130200	-0.93061000	
C	6.80806100	2.42955000	-0.24853900	
C	9.81113000	2.58747700	-2.54209500	
C	8.98184700	2.11784200	2.40813900	
C	11.04785900	2.85255100	1.44450600	
C	6.11383500	-0.25397500	-0.14124300	
C	9.71688000	5.29665500	-1.93127900	
C	5.46256100	2.06827900	-0.24940900	
C	9.99906200	3.53196500	-3.54790900	
C	5.10132900	0.71368200	-0.19476400	
C	9.95292300	4.90711100	-3.25949600	
C	9.46071300	2.43146000	3.68013800	
C	11.54082800	3.16246600	2.70888000	
C	10.75072500	2.95700000	3.85412700	
H	8.22594300	-0.63901400	-0.09105800	
H	9.36292600	4.68086200	0.08609200	
H	7.05951500	3.48315400	-0.30614300	
H	9.84441100	1.53135000	-2.78787000	

H	7.98299700	1.70606500	2.31719100
H	11.68011800	3.04620600	0.58146400
H	5.84663800	-1.30680300	-0.10366300
H	9.68555800	6.35363900	-1.67716500
H	4.70960500	2.84665800	-0.30397200
H	10.18483300	3.20304700	-4.56783700
H	8.82507800	2.26845200	4.54726800
H	12.53945800	3.58066300	2.81097200
H	10.02604200	5.55221400	-5.20392500
H	9.82696800	6.78214000	-4.07993300
H	10.76224100	2.87496700	5.90368200
H	12.21845000	3.37074200	5.22716100
O	10.04638600	0.68794600	-0.49887700
H	10.97399500	0.83579600	-0.27228500
N	-2.11458700	3.12737700	-0.20600500
N	-10.22895100	5.82027900	-4.21184700
N	-8.42878700	8.13333000	5.09602500
C	-6.29258800	7.11578700	-0.17951500
C	-5.19150200	6.04130300	-0.21342600
C	-7.37878200	6.79025300	-1.22381000
C	-6.87564400	7.31104800	1.23277500
C	-3.83665600	6.39506000	-0.16890200
C	-8.53872900	6.06682000	-0.91405900
C	-5.50924800	4.67644900	-0.26062900
C	-7.18348300	7.15830900	-2.56348900
C	-6.29802600	6.75854700	2.38297800
C	-7.97850700	8.16416400	1.41497700
C	-2.83859200	5.42149500	-0.17047600
C	-9.46997700	5.72689500	-1.89593300
C	-4.52222000	3.69326600	-0.25448400
C	-8.10883300	6.82951800	-3.55083900
C	-3.16880900	4.05988600	-0.20923800
C	-9.27038000	6.10385000	-3.23372600
C	-6.79490000	7.03722200	3.65623500
C	-8.47931800	8.45674300	2.68037100
C	-7.89327900	7.89425600	3.82851500
H	-3.56380200	7.44257500	-0.13834800
H	-8.73100600	5.76462000	0.11084900
H	-6.54708500	4.36502100	-0.31118400
H	-6.29072500	7.71334600	-2.83147000
H	-5.44268800	6.09824300	2.29345700
H	-8.47223000	8.60041900	0.55008300
H	-1.79345700	5.71823300	-0.14042500
H	-10.36448700	5.17346500	-1.61965600
H	-4.81873900	2.65105300	-0.29541300
H	-7.93234900	7.13821900	-4.57870500
H	-6.32604600	6.58262900	4.52573600
H	-9.33981800	9.11396200	2.78129400
H	-9.89185600	5.80965500	-5.16490200

H	-10.83922600	5.03893800	-4.01421200
H	-7.80476000	7.97930300	5.87600200
H	-8.97016900	8.98087500	5.19597500
O	-5.62770100	8.34645300	-0.56105000
H	-6.21494900	9.07974600	-0.33499200
H	-2.42652000	-2.71816200	-0.22161500
C	-0.45300700	-2.80053100	-0.21683200
H	0.43505900	-3.42399100	-0.21442200
N	-1.64980500	-3.39501000	-0.22192400
N	0.12331300	-11.79767200	-4.15010800
N	-2.88745500	-11.32730700	5.11883900
C	-3.01546500	-9.00731200	-0.17549500
C	-2.63576800	-7.51660900	-0.21585600
C	-2.17742700	-9.79236000	-1.20416300
C	-2.90896300	-9.59923200	1.24250600
C	-3.61985100	-6.51971800	-0.19674300
C	-0.97358100	-10.43091100	-0.87567300
C	-1.29416300	-7.10974400	-0.24363600
C	-2.57862800	-9.81879300	-2.54827100
C	-2.73291600	-8.81430500	2.38915400
C	-3.09770200	-10.97967500	1.43257000
C	-3.27535200	-5.16864300	-0.20335600
C	-0.20196600	-11.07469500	-1.84364700
C	-0.93595800	-5.76347000	-0.24183100
C	-1.81944700	-10.46293600	-3.52189300
C	-1.93049900	-4.77421900	-0.22160500
C	-0.61314400	-11.10196200	-3.18595800
C	-2.74020900	-9.37467600	3.66650700
C	-3.11478800	-11.55047600	2.70202600
C	-2.93428700	-10.75327100	3.84657200
H	-4.66394700	-6.80654300	-0.18162600
H	-0.62674000	-10.43733700	0.15311300
H	-0.50493900	-7.85324000	-0.27378800
H	-3.50314800	-9.32645700	-2.83067300
H	-2.58765100	-7.74412000	2.29346400
H	-3.21792800	-11.63167400	0.57085000
H	-4.05511000	-4.41158700	-0.19278300
H	0.72197100	-11.56920200	-1.55284000
H	0.11555700	-5.49984500	-0.26512800
H	-2.16340800	-10.47319500	-4.55365800
H	-2.59118300	-8.73495100	4.53314000
H	-3.25394500	-12.62367000	2.80913800
H	-0.02581400	-11.50877100	-5.10737300
H	1.10301600	-11.93266400	-3.94046100
H	-3.07509500	-10.70448700	5.89238000
H	-3.35073300	-12.21978500	5.22011900
O	-4.40892600	-9.05093100	-0.57321300
H	-4.75301400	-9.92373800	-0.34201900

B precursor				Optimized structure
O 1				
N	-1.17904000	5.37930900	-0.83840100	
N	-4.26827600	-3.54873500	-0.78100700	
N	5.30555200	-1.78829800	-0.77641700	
C	0.03076500	-0.02591700	0.81816300	
C	-0.31039800	1.40817300	0.37987300	
C	-1.08197400	-0.99928100	0.38248600	
C	1.42033100	-0.47698900	0.32660000	
C	-0.04825700	2.49885500	1.22025300	
C	-1.03180800	-1.72461400	-0.81561200	
C	-0.85249800	1.67993000	-0.88371100	
C	-2.23733300	-1.12659800	1.16809700	
C	2.33787300	0.39100200	-0.27797800	
C	1.84716800	-1.79526700	0.56605200	
C	-0.31693800	3.80723500	0.81776300	
C	-2.08567700	-2.54814800	-1.21475400	
C	-1.11689900	2.98384000	-1.29891900	
C	-3.29226700	-1.95035800	0.78335100	
C	-0.85364800	4.07321700	-0.45188900	
C	-3.23513400	-2.67592500	-0.41926000	
C	3.62110300	-0.03032000	-0.62872700	
C	3.12707600	-2.22651500	0.22847300	
C	4.04036300	-1.34595000	-0.37807600	
H	0.36600600	2.31771600	2.20484600	
H	-0.15578600	-1.65583800	-1.45323500	
H	-1.08127500	0.86379800	-1.56128300	
H	-2.30449600	-0.56941900	2.09649900	
H	2.05247200	1.41706600	-0.48112700	
H	1.16135800	-2.51237900	1.01104000	
H	-0.11406900	4.63079600	1.49889300	
H	-2.01006900	-3.10493000	-2.14603900	
H	-1.54554400	3.15822300	-2.28319300	
H	-4.16994700	-2.03487100	1.42031300	
H	4.30401600	0.66972900	-1.10457800	
H	3.41826700	-3.25641500	0.42157800	
H	-1.22450000	5.54091500	-1.83536600	
H	-0.67833600	6.11376400	-0.35672400	
H	-5.17178000	-3.34548500	-0.37520900	
H	-4.33435900	-3.76116300	-1.76727000	
H	6.00556800	-1.06845600	-0.89314800	
H	5.66439300	-2.59539600	-0.28488200	
O	0.06815600	0.02311400	2.26843100	
H	0.49410000	-0.78673800	2.57909900	
A precursor				Optimized structure

0 1				
O	-2.51734700	2.70198300	0.00000000	
O	3.59866200	0.82913700	0.00000000	
O	-1.08128600	-3.53110900	0.00000000	
C	-1.23995100	0.71376000	0.00000000	
C	1.23811400	0.71694200	0.00000000	
C	0.00183100	-1.43073100	0.00000000	
C	0.00000000	1.41066600	0.00000000	
C	-1.22167300	-0.70534600	0.00000000	
C	1.22167400	-0.70534200	0.00000000	
C	-2.47988600	1.45870800	0.00000000	
C	2.50321200	1.41830500	0.00000000	
C	-0.02332200	-2.87702000	0.00000000	
H	-3.41704900	0.88552900	0.00000000	
H	2.47539700	2.51650300	0.00000000	
H	0.94166000	-3.40202000	0.00000000	
O	-2.37599300	-1.35450000	0.00000000	
H	-2.16100700	-2.34093200	0.00000000	
O	2.36104900	-1.38037200	0.00000000	
H	3.10776300	-0.70088400	0.00000000	
O	0.01493000	2.73489700	0.00000000	
H	-0.94688300	3.04186200	0.00000000	

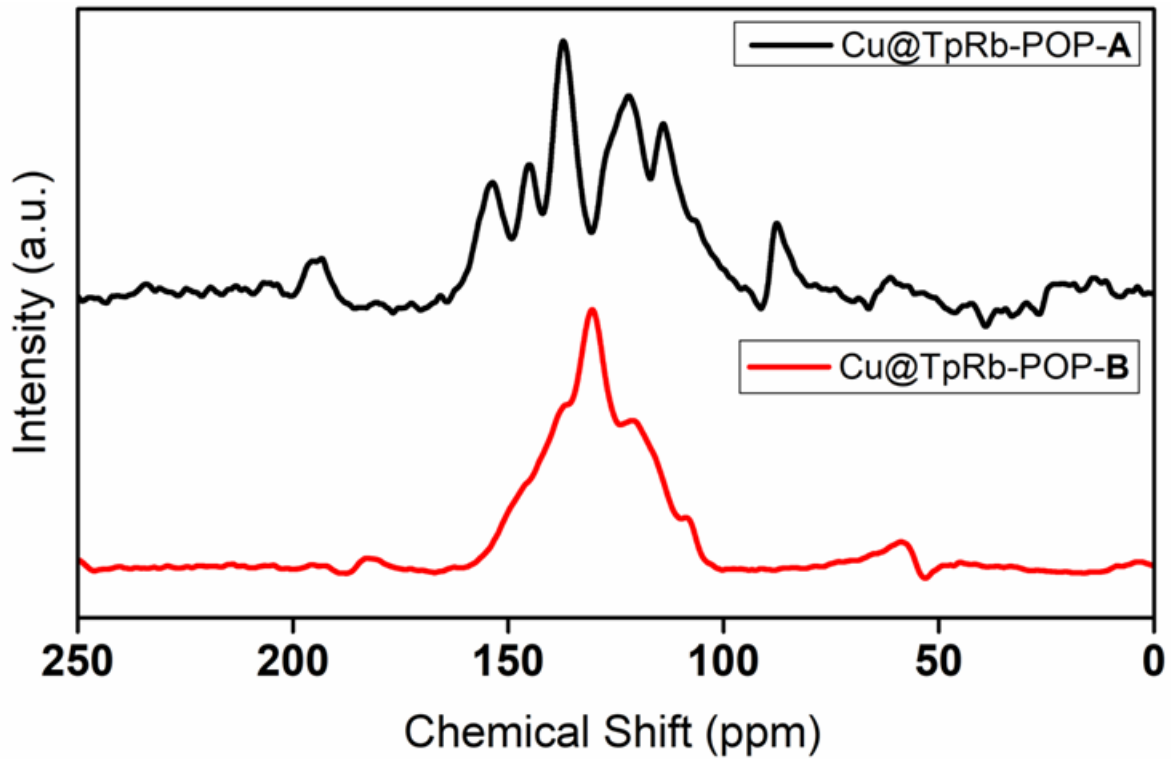


**Figure S4:**  $^{13}\text{C}$  Cross Polarization (CP) solid state MAS NMR spectra of the respective Cu@TpRb-POP materials.

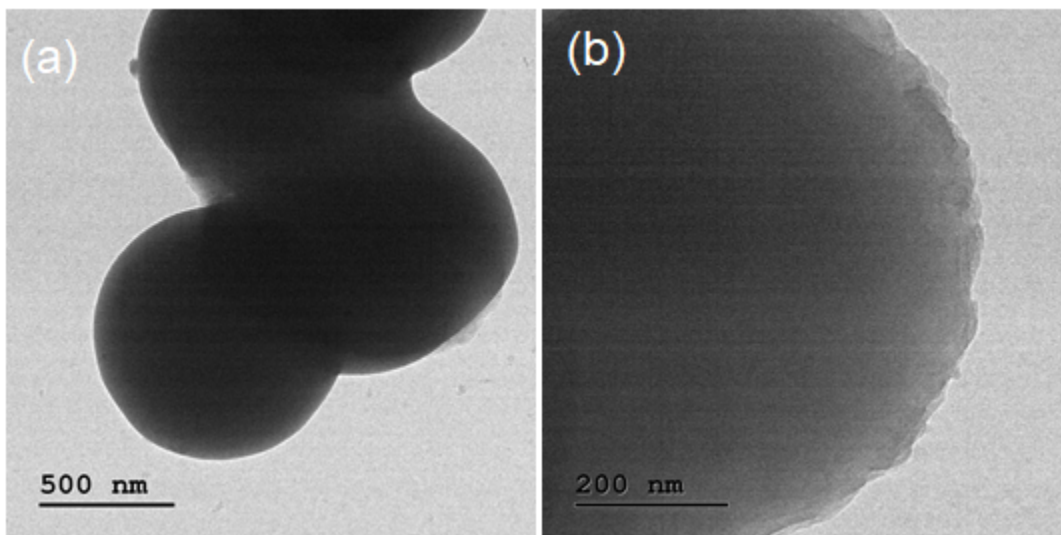


**Figure S5:** TEM images in different magnifications of TpRb-POP.

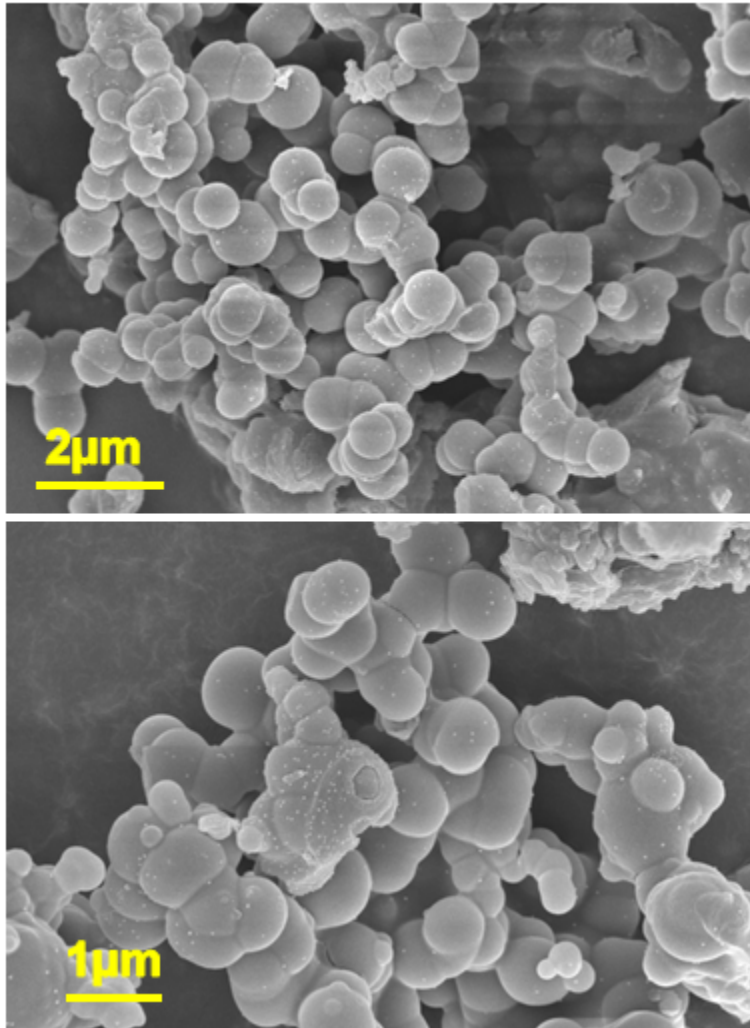


**Figure S6:** FE-SEM images in different magnifications of Cu@TpRb-POP-A.

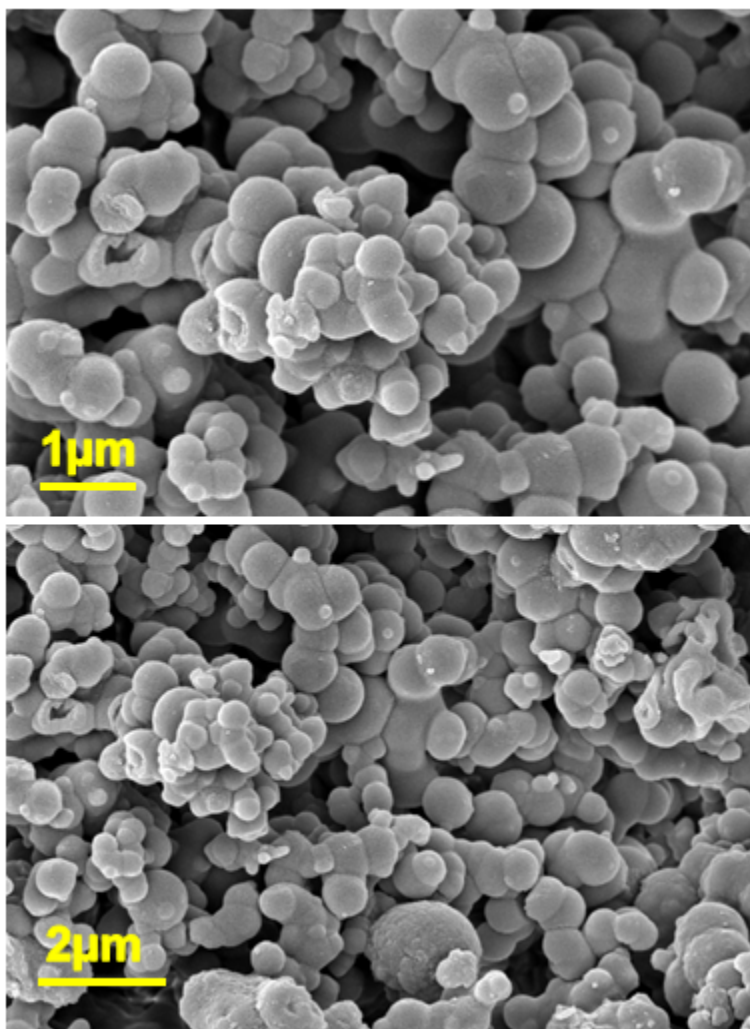


**Figure S7:** FE-SEM images in different magnifications of Cu@TpRb-POP-B.

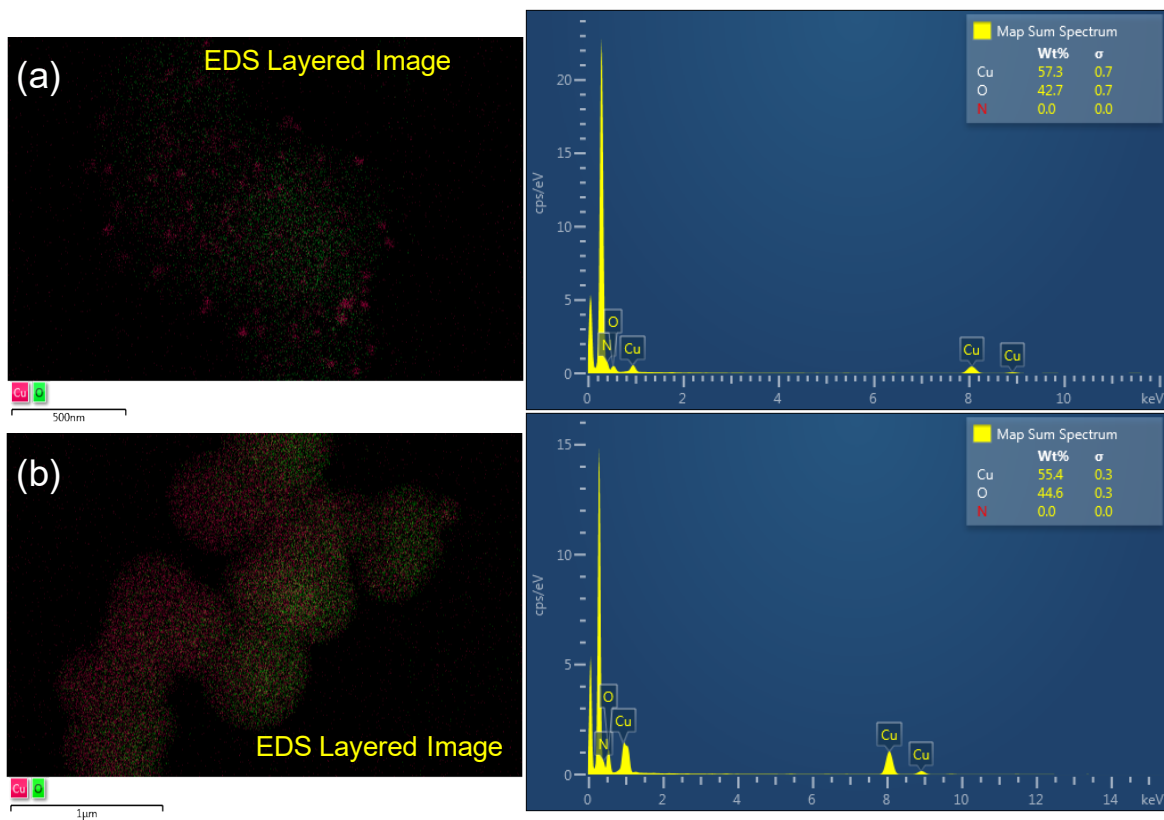


**Figure S8:** Energy dispersive X-ray (EDX) spectroscopy of Cu@TpRb-POP-A (a) & Cu@TpRb-POP-B (b), respectively.

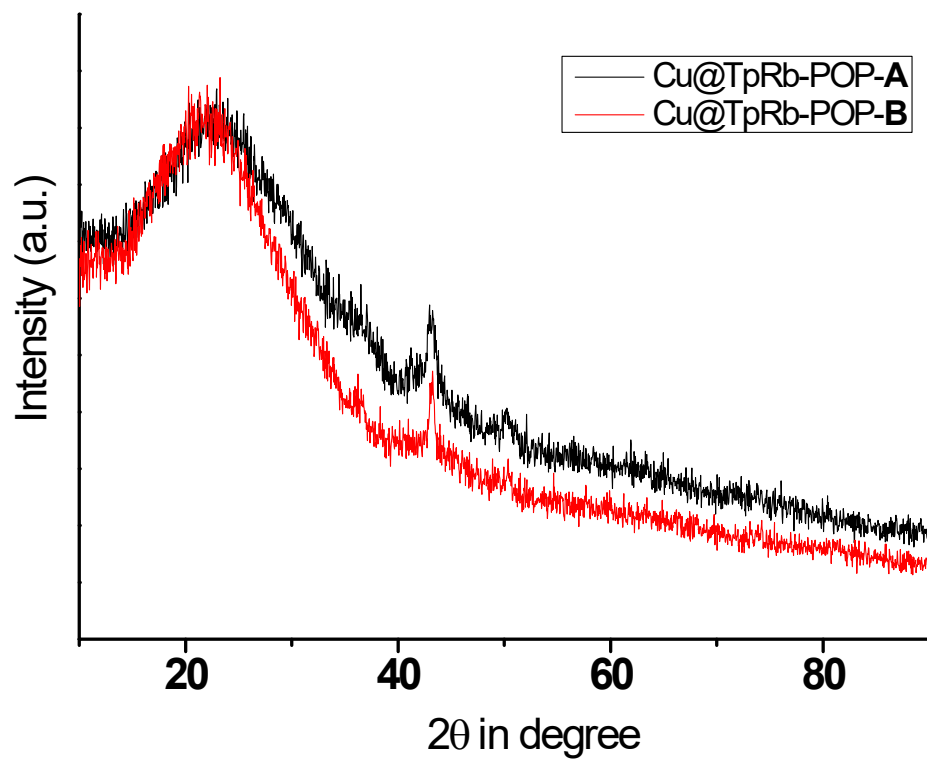


**Figure S9:** Wide angle powder X-ray diffraction patterns of Cu@TpRb-POP-A & Cu@TpRb-POP-B, respectively.

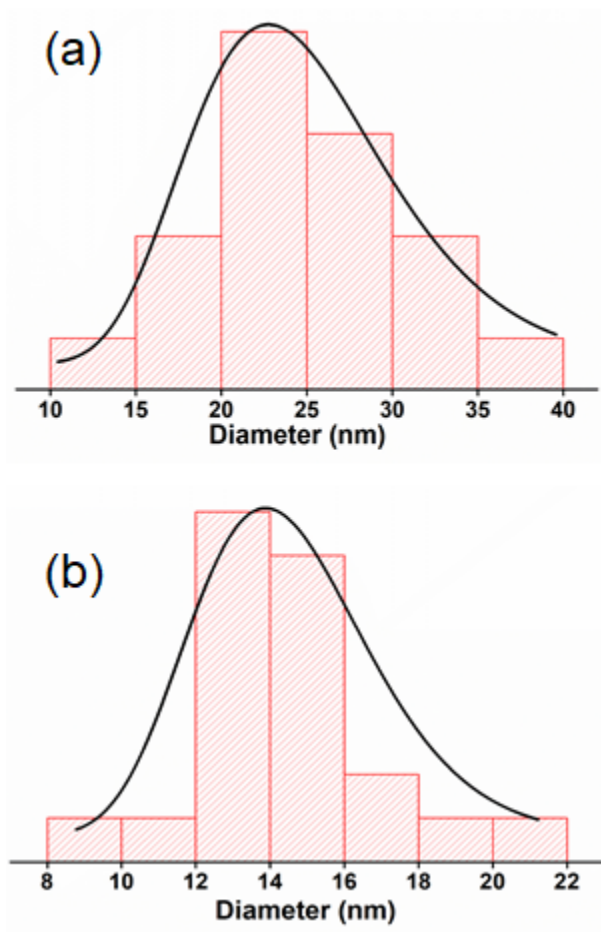


**Figure S10:** Particle size distribution histogram profile of as synthesized Cu@TpRb-POP-A (a) & Cu@TpRb-POP-B (b), respectively.

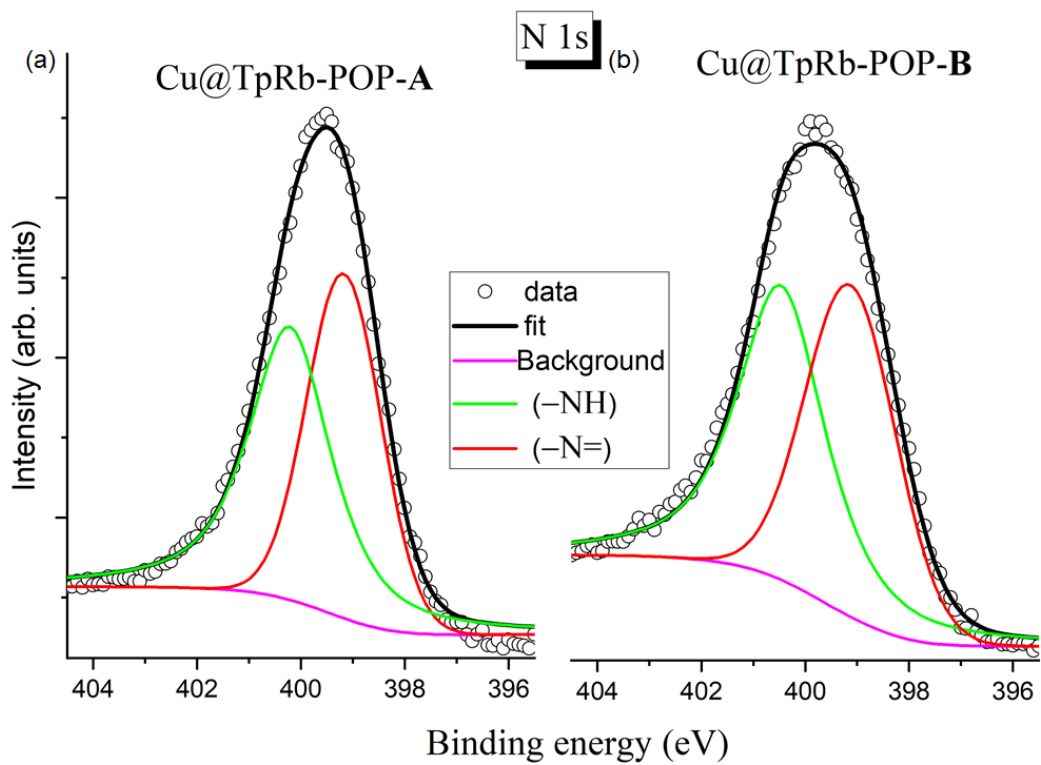


**Figure S11:** N-1s X-ray photoelectron spectra (XPS) of Cu@TpRb-POP-A (a) & Cu@TpRb-POP-B (b), respectively.

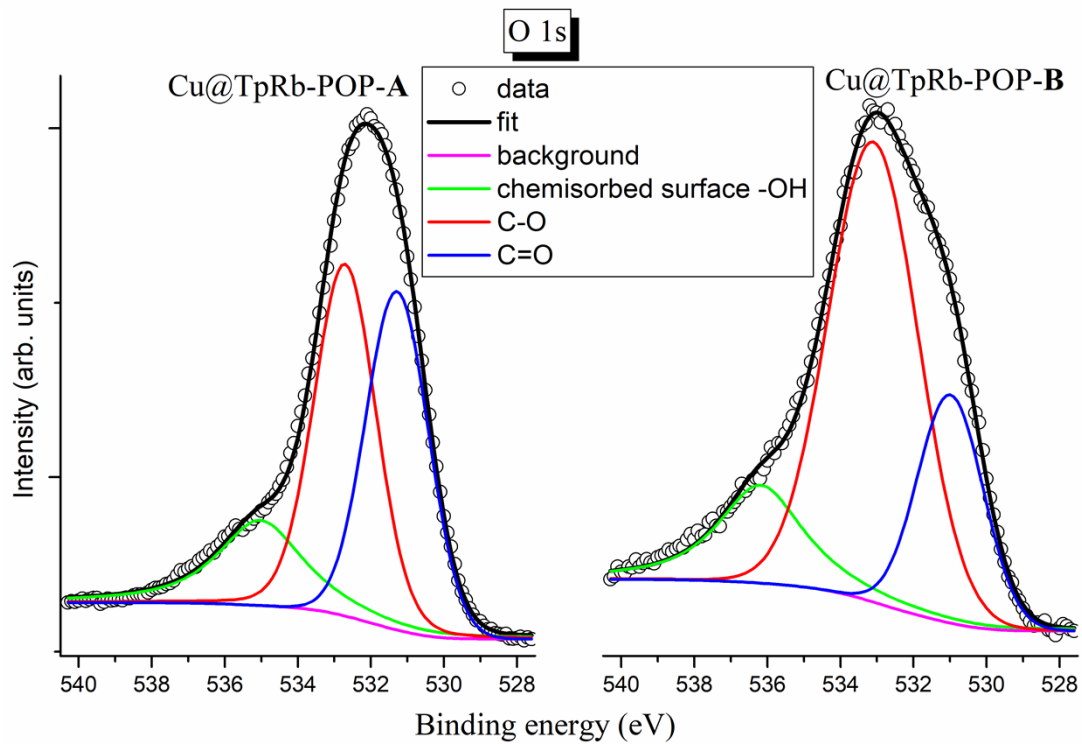


**Figure S12:** O-1s X-ray photoelectron spectra (XPS) of Cu@TpRb-POP-A (a) & Cu@TpRb-POP-B (b), respectively.

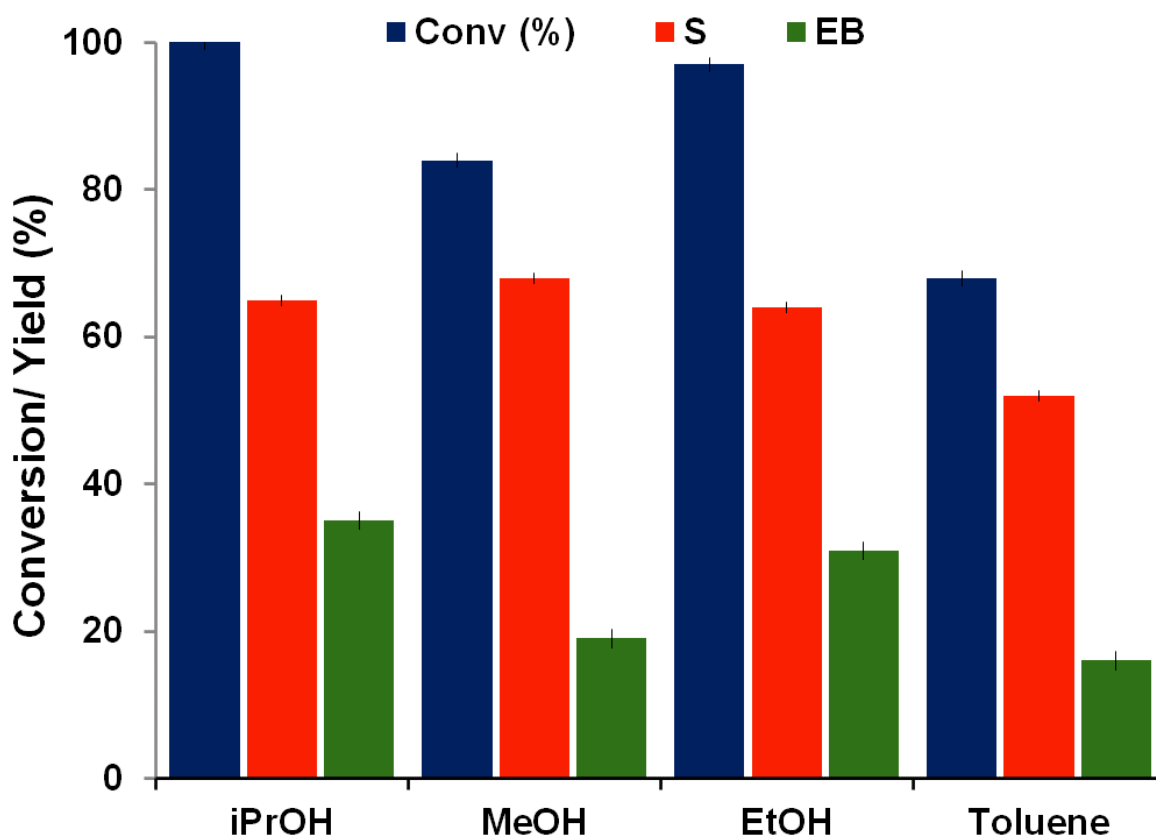


**Figure S13:** Evolution of reactant and product distributions against time in other solvents for Cu@TpRb-POP-A catalysts under optimized reaction conditions. **Reaction conditions:** Phenyl Acetylene (PA) (0.11ml, 1 mmol), Cu-catalyst (30 mg), solvent (30 mL), H<sub>2</sub> pressure (20 bar), Reaction temperature (150 °C), Time (10 h).

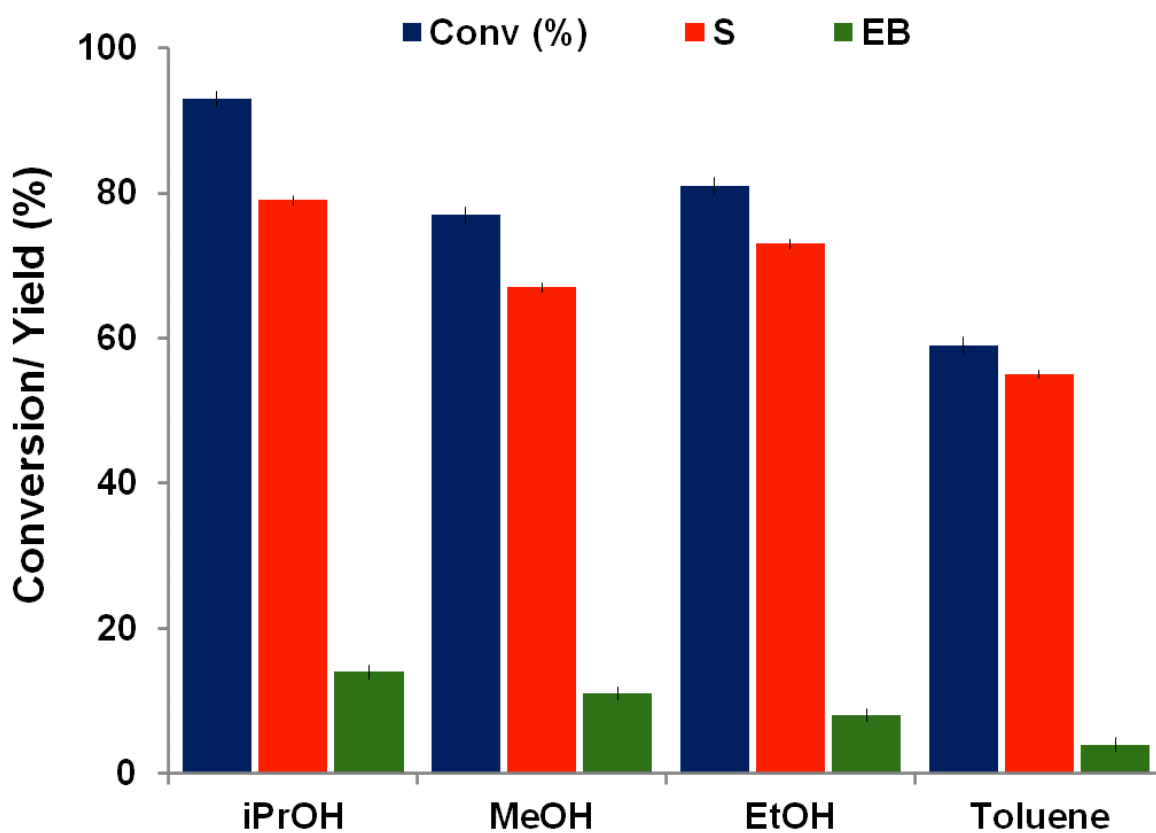


**Figure S14:** Evolution of reactant and product distributions against time in other solvents for Cu@TpRb-POP-B catalysts under optimized reaction conditions. **Reaction conditions:** Phenyl Acetylene (PA) (0.11ml, 1 mmol), Cu-catalyst (30 mg), solvent (30 mL), H<sub>2</sub> pressure (20 bar), Reaction temperature (150 °C), Time (10 h).

**Table S3:** Comparison of Seminal Hydrogenation of Phenyl Acetylene catalytic performance with various Cu catalysts under optimized reaction conditions.

<b>Entry</b>	<b>Catalyst Used</b>	<b>Con (%)</b>	<b>Styrene Yield (%)</b>	<b>Ethyl Benzene Yield (%)</b>
<b>1.</b>	Cu(NO <sub>3</sub> ) <sub>2</sub> ·3H <sub>2</sub> O	12.3	9.6	2.7
<b>2.</b>	Cu-NPs	21.6	15.9	5.7
<b>3.</b>	Cu-DVAC-1	75.8	63.1	12.7
<b>4.</b>	Cu-SBA-15	65.4	58.2	7.2
<b>5.</b>	Cu@TpRb-POP-B	93.2	80.1	13.1

**Reaction conditions:** Phenyl Acetylene (PA) (0.11ml, 1 mmol), Cu-catalysts (30 mg), isopropanol (30 mL), H<sub>2</sub> pressure (20 bar), Reaction temperature (150 °C), Time (10 h).

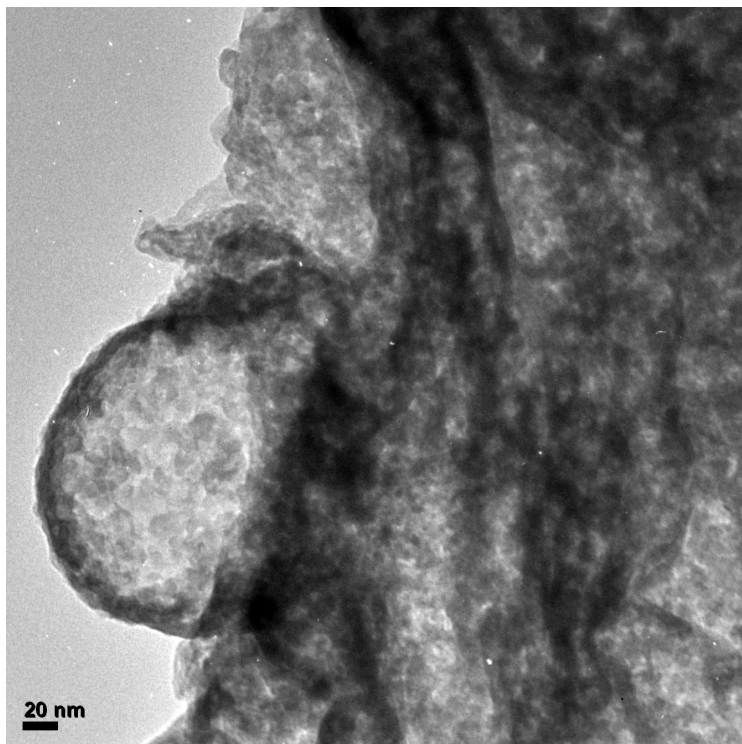


**Figure S15:** TEM image of Cu-DVAC-1 Catalyst

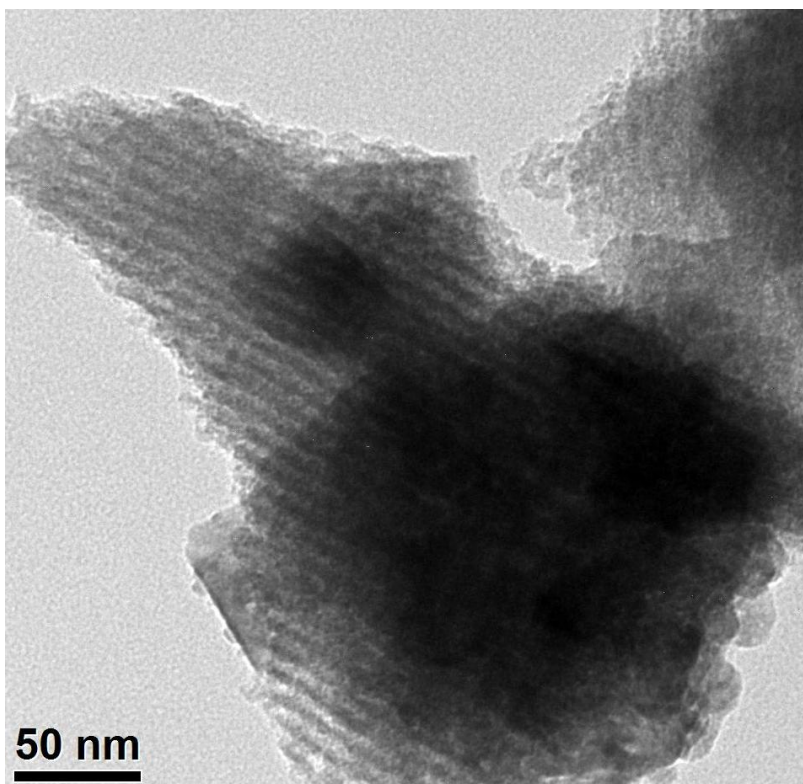


**Figure S16:** TEM image of Cu-SBA-15 Catalyst

**Table S4:** Comparison of Seminal Hydrogenation of Phenyl Acetylene catalytic performance with carbon supported Cu catalysts under optimized reaction conditions.

<b>Entry</b>	<b>Catalyst Used</b>	<b>Con (%)</b>	<b>Styrene Yield (%)</b>	<b>Ethyl Benzene Yield (%)</b>
<b>1.</b>	Cu@C-A	76.5	71.2	5.1
<b>2.</b>	Cu@C-B	72.3	67.4	4.9
<b>3.</b>	Cu@TpRb-POP-A	99.1	65.3	33.8
<b>4.</b>	Cu@TpRb-POP-B	93.2	80.1	13.1

**Reaction conditions:** Phenyl Acetylene (PA) (0.11ml, 1 mmol), Cu-catalysts (30 mg), isopropanol (30 mL), H<sub>2</sub> pressure (20 bar), Reaction temperature (150 °C), Time (10 h).

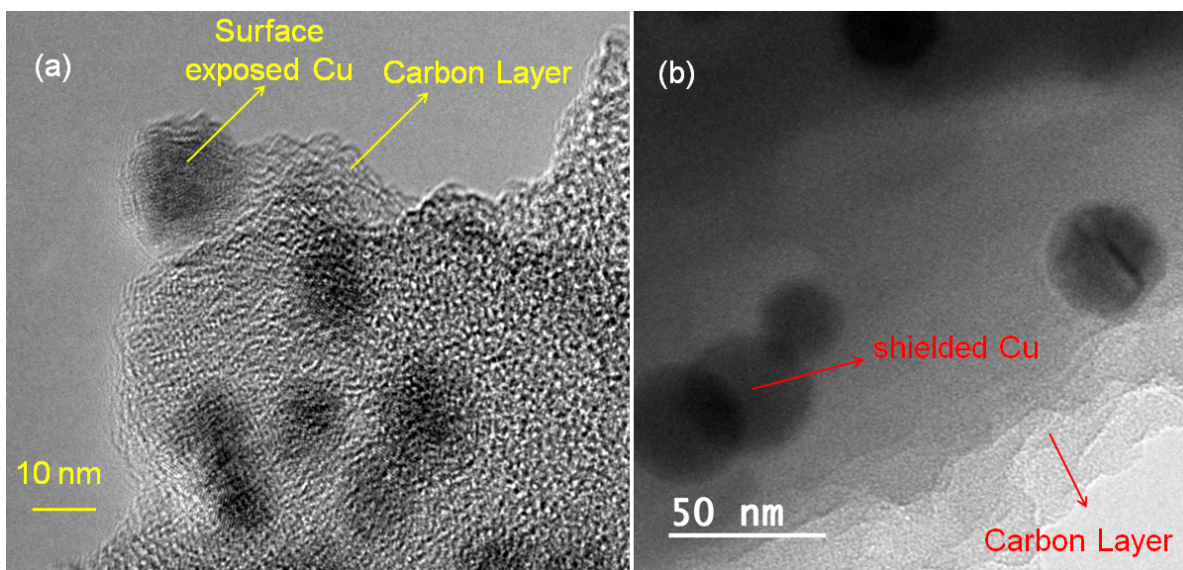


**Figure S17:** TEM images of Cu@C-A (a) & Cu@C-B (b) catalysts, respectively.

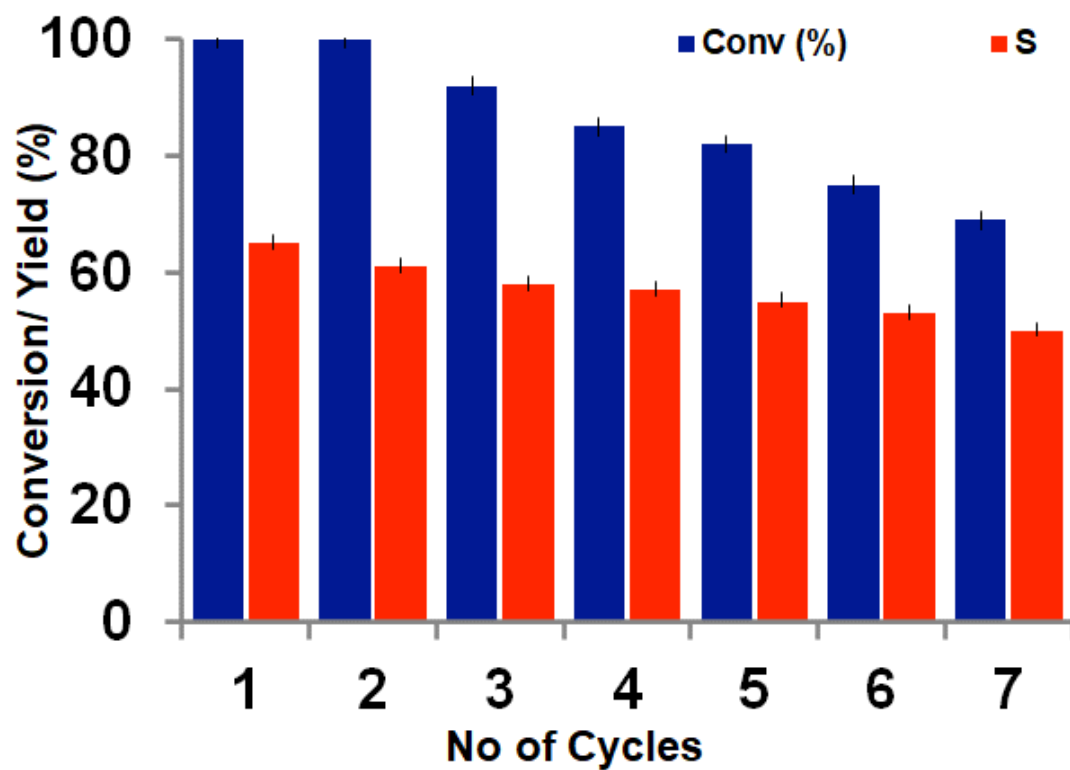


**Figure S18:** Recyclability test for Cu@TpRb-POP-A catalyst under optimized reaction conditions. **Reaction conditions:** Phenyl Acetylene (PA) (0.11ml, 1 mmol), Cu-catalysts (30 mg), isopropanol (30 mL), H<sub>2</sub> pressure (20 bar), Reaction temperature (150 °C), Time (10 h).

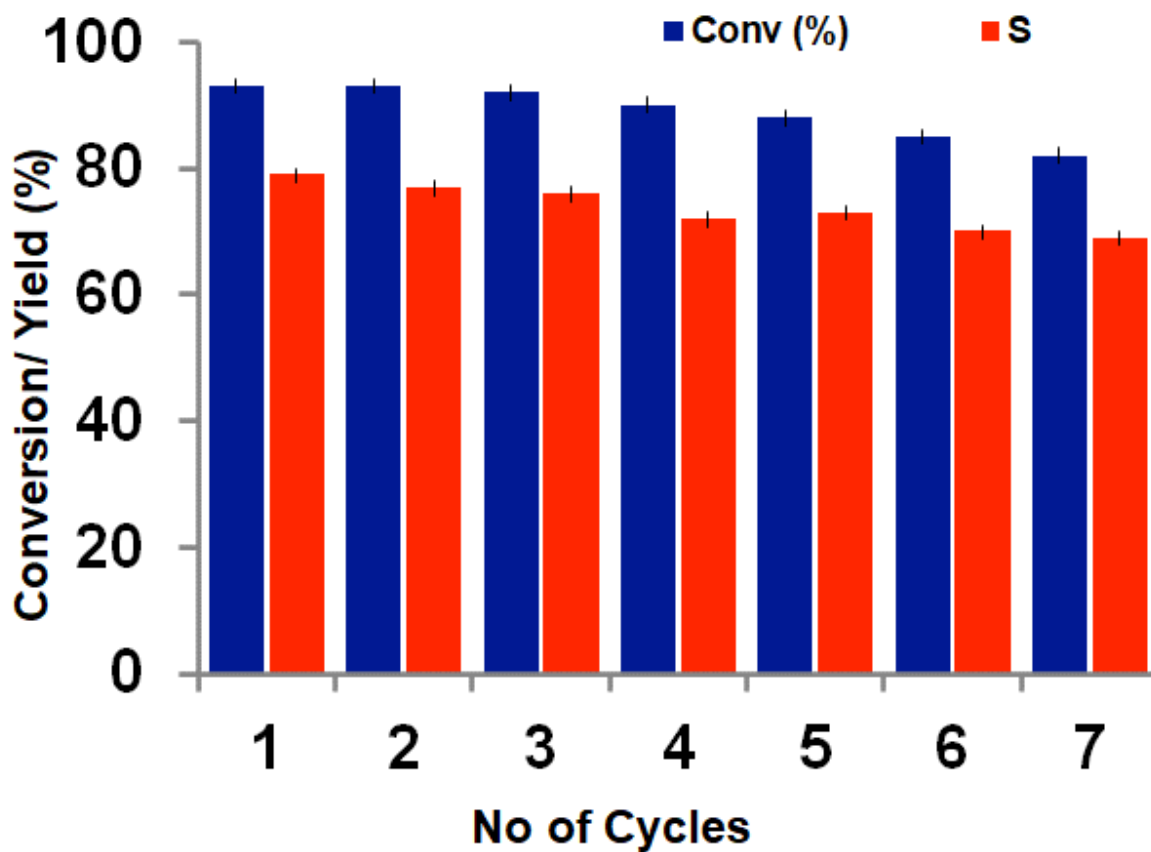


**Figure S19:** Recyclability test for Cu@TpRb-POP-B (b) catalyst under optimized reaction conditions. **Reaction conditions:** Phenyl Acetylene (1ml, 10 mmol), catalyst (200 mg), and isopropanol (150 mL), 150°C temperature, 20 bar H<sub>2</sub> pressure, Time 10 h.

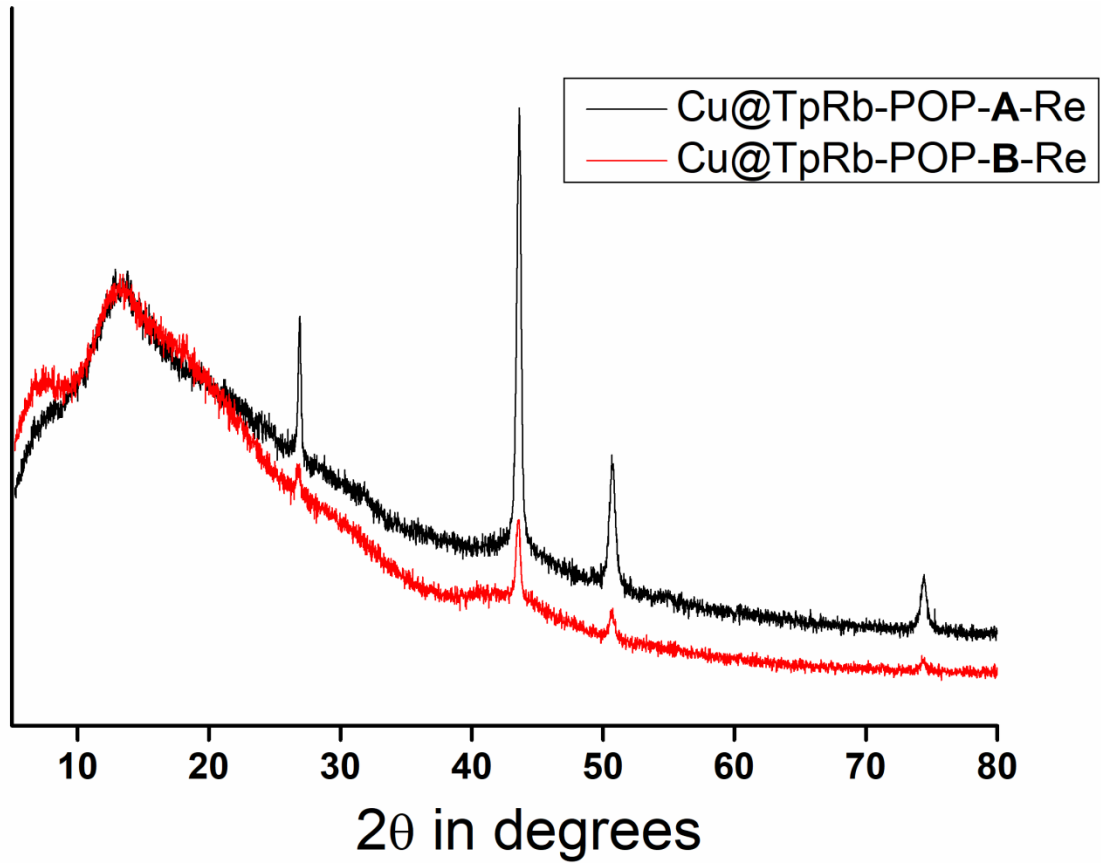


**Figure S20:** Wide angle Powder X-ray diffraction patterns of reused Cu@TpRb-POP-A & Cu@TpRb-POP-B, respectively.

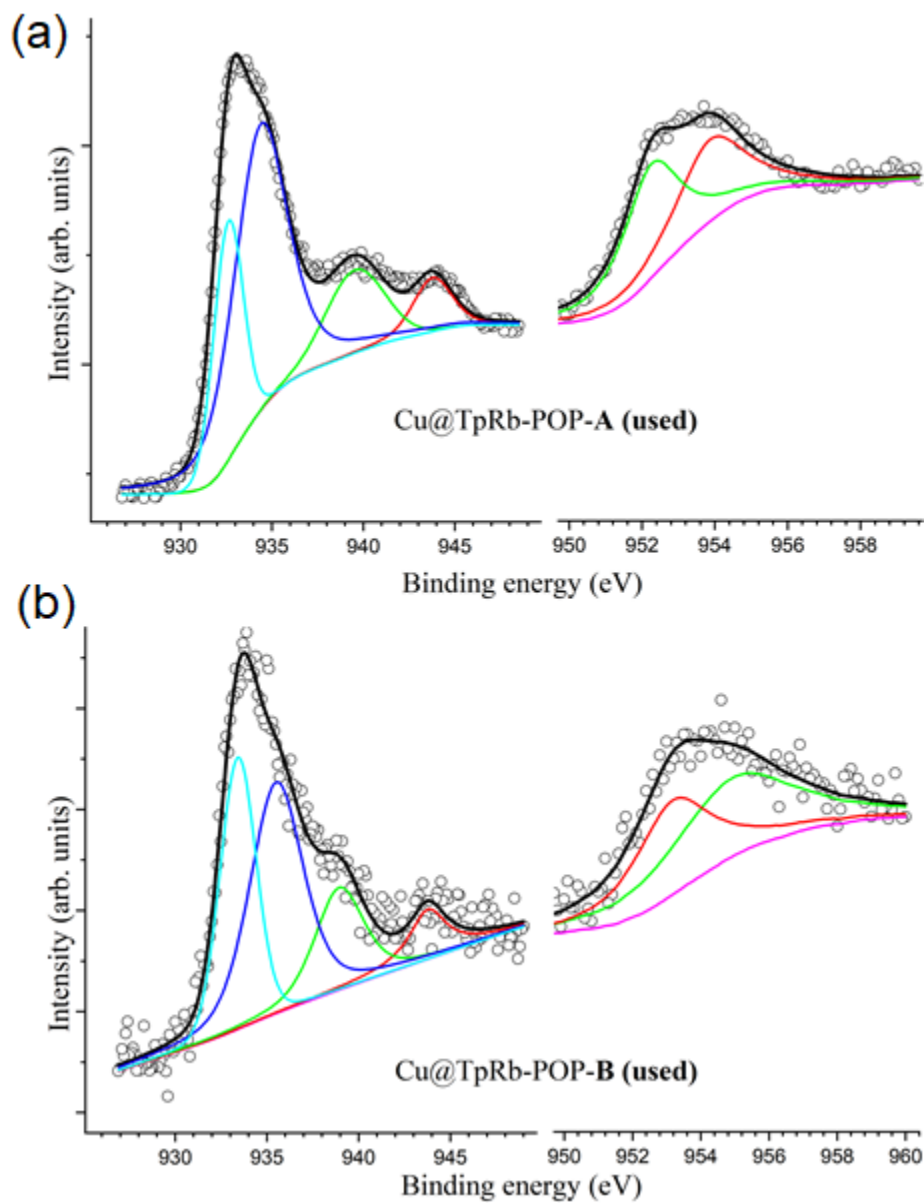


**Figure S21:** XP-spectra of reused Cu@TpRb-POP-A (a) & Cu@TpRb-POP-B (b) catalysts, respectively.

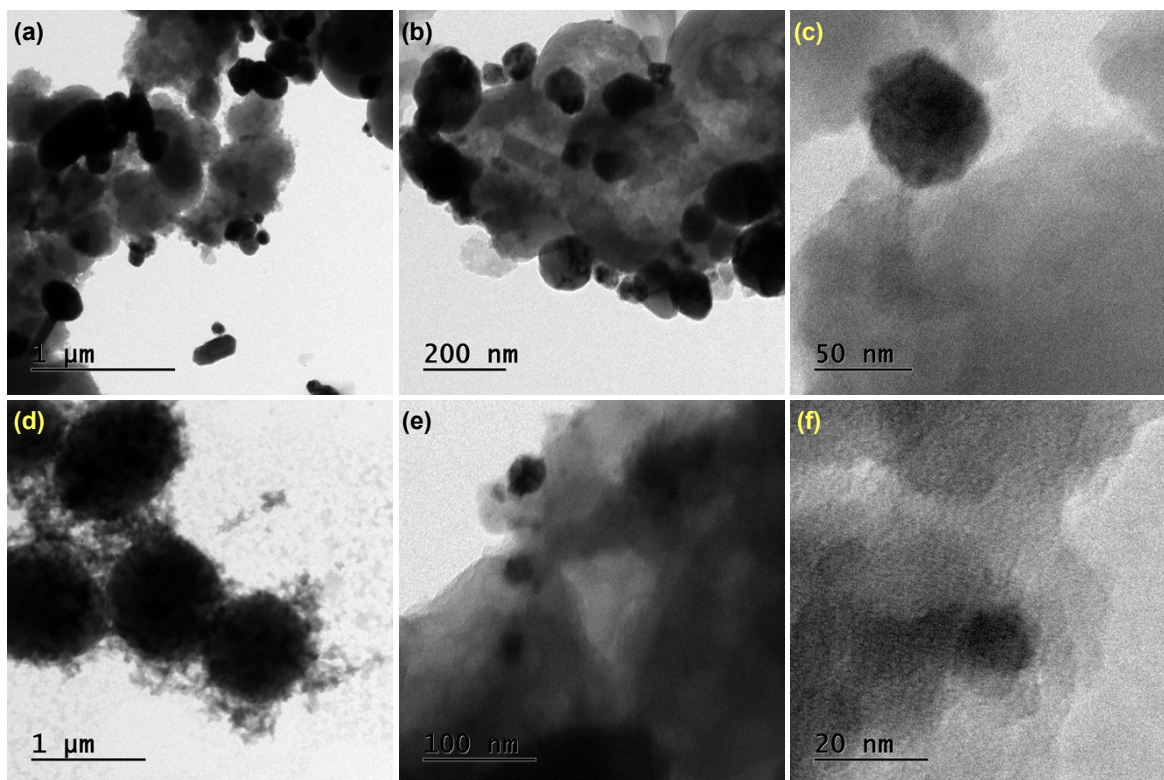


**Figure S22:** TEM image of reused Cu@TpRb-POP-A (a, b, & c) & Cu@TpRb-POP-B (d, e & f) catalysts, respectively.

**Table S5:** Adsorption energies ( $E_{\text{ads}}$ ) of phenylacetylene, styrene and ethylbenzene on the geometrically optimized structures of Cu@TpRb-POP-A and Cu@TpRb-POP-B.

	<b>Phenylacetylene (eV)</b>	<b>Styrene (eV)</b>	<b>Ethyl benzene (eV)</b>
<b>Cu@TpRb-POP-A</b>	-2.58	-1.51	-1.40
<b>Cu@TpRb-POP-B</b>	-1.60	-1.15	-1.11

$$E_{\text{ads}} = E(\text{Cu@TpRb-POP} + \text{Alkyne/Alkene/Alkane}) - E(\text{Cu@TpRb-POP}) - E(\text{Alkyne/Alkene/Alkane})$$

where  $E(\text{Cu@TpRb-POP} + \text{Alkyne/Alkene/Alkane})$  is the energy of adsorbed system,  $E(\text{Cu@TpRb-POP})$  is the energy of Cu@TpRb-POP (**A** or **B**) and  $E(\text{Alkyne/Alkene/Alkane})$  is the energy of alkyne, alkene or alkane.

**Table S6:** Comparison study with other reported catalysts for Semi hydrogenation of alkyne.

Entry	Catalytic System	Reaction Condition	Alkyne Conversion (%)	Alkene Selectivity (%)	Reference
1	Cy <sub>3</sub> P-Cu/SiO <sub>2</sub> - 700	50bar H <sub>2</sub> , 60 °C, toluene, 24 h, Reactant 400μmol	100	94	12
2	10-CuPd	Gas Phase, 100 °C	94	15	13
3	Cu <sub>2.75</sub> Ni <sub>0.25</sub> Fe	H <sub>2</sub> /C <sub>3</sub> H <sub>4</sub> /He= 7.5/2.5/90, P=1 bar, T=250 °C, Reactant 1mmol	100	97	14
4	Ru <sub>3</sub> (CO) <sub>12</sub> / TPPTS	CO/ H <sub>2</sub> (10bar), EG-Toluene 1:1 (10 mL), 80 °C, 10 h, Reactant 0.5 mmol	100	94	15
5	Cu NPs	KOH (2 mmol), TH (15 ml), 150 °C, Reactant 1mmol	96	95	16

6	Mn(I)-PNP Complex	KO <sup>t</sup> Bu, 30 bar H <sub>2</sub> , 60 °C, 16 h, Reactant 0.5 mmol	99	88	17
7	PyC <sub>12</sub> S-Pd/VC	30 °C, DCM, 1bar, Reactant 1mmol	100	90	18
8	Pd@Ag	Room temperature, EtOH, 50 bar, 1h, Reactant 0.3 mmol	>99	>99	19
9	PdCuS	Room temperature, cyclohexane with H <sub>2</sub> O, 2h, Reactant 0.5 mmol	> 99	97	20
10	N-heterocyclic carbene modified Cu/SiO <sub>2</sub>	60 °C, Toluene, 20 bar, 16h, Reactant 400μmol	100	95	21
12	<b>Cu@TpRb-POP-B</b>	<b>150 °C, 20 bar, 10 h, iPrOH, Reactant 1 mmol</b>	93	74	<b>Our Work</b>

To understand the efficiency of our as-synthesized Cu catalyst, we have compared thoroughly the catalytic activity with the previously reported catalyst and included it in Table S6, SI.  $\text{Cy}_3\text{P-Cu/SiO}_{2-700}$  catalyst (Entry 1, Table S6, SI) synthesized by Fedorov *et al.* exhibited excellent alkyne conversion and alkene selectivity, under very high pressure (50 bar) which is not a greener approach for hydrogenation.<sup>12</sup> On the other hand 10-CuPd (bimetallic system) showed good alkyne conversion but poor alkene selectivity.<sup>13</sup> Another catalytic system developed by Bridieret *et. al* (Entry 3, Table S6, SI) exhibited good alkyne hydrogenation, but again the reaction conditions were too harsh.<sup>14</sup> Another catalytic system using noble metal  $\text{PyC}_{12}\text{S-Pd/VC}$  reported by Yoshii *et al.*<sup>18</sup> exhibited good conversion and selectivity. Some other homogeneous system like  $\text{Ru}_3(\text{CO})_{12}/\text{TPPTS}$ ,<sup>15</sup> Cu NPs<sup>16</sup> and Mn(I)-PNP Complex<sup>17</sup> had been reported earlier for semi hydrogenation of alkyne, but most of them used harsh reaction conditions and noble metal, which is not desirable. Comparatively, our catalyst Cu@TpRb-POP-B (Entry 12, Table S6, SI) a non-noble metal-based system exhibited excellent activity (93% conversion, 74% selectivity) under low pressure (20 bar) and low reaction temperature (150 °C) and reusability (negligible change in activity after the 7<sup>th</sup> cycle). The superior activity of our catalyst originated from the access restriction of the reactant molecule to the catalytic center which prevents the over hydrogenation of alkynes to alkane.

## References:

- (1) Frisch, M. J.; Trucks, G. W.; Schlegel, H. B.; Scuseria, G. E.; Robb, M. A.; Cheeseman, J. R.; Scalmani, G.; Barone, V.; Petersson, G. A.; Nakatsuji, H.; et al. Gaussian 16 Rev. A.03. Gaussian Inc. Wallingford CT 2016.
- (2) Becke, A. D. Density-Functional Thermochemistry. III. The Role of Exact Exchange. *J. Chem. Phys.* **1993**, *98* (7), 5648. <https://doi.org/10.1063/1.464913>.
- (3) Ngo, T. C.; Dao, D. Q.; Nguyen, M. T.; Nam, P. C. A DFT Analysis on the Radical Scavenging Activity of Oxygenated Terpenoids Present in the Extract of the Buds of *Cleistocalyx Operculatus*. *RSC Adv.* **2017**, *7*, 39686-39698. <https://doi.org/10.1039/C7RA04798C>.

- (4) Tirado-Rives, J.; Jorgensen, W. L. Performance of B3LYP Density Functional Methods for a Large Set of Organic Molecules. *J. Chem. Theory Comput.* **2008**, *4*, 297-306. <https://doi.org/10.1021/ct700248k>.
- (5) G. Kresse and J. Furthmüller, Efficiency of ab-initio total energy calculations for metals and semiconductors using a plane-wave basis set, *Computational Materials Science* **1996**, *6*, 15-50.
- (6) G. Kresse and D. Joubert, From ultrasoft pseudopotentials to the projector augmented-wave method, *Physical Review B* **1999**, *59*, 1758.
- (7) J. P. Perdew, K. Burke and M. Ernzerhof, Generalized Gradient Approximation Made Simple, *PHYSICAL REVIEW LETTERS* **1996**, *77*, 3865.
- (8) A. Tkatchenko and M. Scheffler, Accurate Molecular Van Der Waals Interactions from Ground-State Electron Density and Free-Atom Reference Data, *Phys. Rev. Lett.* **2009**, *102*, 073005.
- (9) A. Tkatchenko, R. A. DiStasio, R. Car and M. Scheffler, Accurate and Efficient Method for Many-Body van der Waals Interactions, *Phys. Rev. Lett.* **2012**, *108*, 236402.
- (10) S. Lee, S. J. Shin, H. Baek, Y. Choi, K. Hyun, M. Seo, K. Kim, D. Y. Koh, H. Kim and M. Choi, Dynamic metal-polymer interaction for the design of chemoselective and long-lived hydrogenation catalysts, *Sci. Adv.* **2020**, *6*.
- (11) Y. Song, R. Ma, L. Hao, X. Yang, C. Wang, Q. Wu and Z. Wang, Application of covalent organic framework as the adsorbent for solid-phase extraction of trace levels of pesticide residues prior to high-performance liquid chromatography-ultraviolet detection, *Journal of Chromatography A*, 2018, **1572**, 20-26.
- (12) Fedorov, A.; Liu, H. J.; Lo, H. K.; Coperet, C. Silica-Supported Cu Nanoparticle Catalysts for Alkyne Semihydrogenation: Effect of Ligands on Rates and Selectivity. *J. Am. Chem. Soc.* **2016**, *138*, 16502-16507. DOI: 10.1021/jacs.6b10817.
- (13) McCue, A. J.; McRitchie, C. J.; Shepherd, A. M.; Anderson, J. A. Cu/Al<sub>2</sub>O<sub>3</sub> catalysts modified with Pd for selective acetylene hydrogenation. *J. Catal.* **2014**, *319*, 127-135. DOI: 10.1016/j.jcat.2014.08.016.
- (14) Bridier, B.; Ramirez, J. P.; Gericke, A. K.; Schlögl, R.; Teschner, D. Surface state during activation and reaction of high-performing multi-metallic alkyne hydrogenation catalysts. *Chem. Sci.* **2011**, *2*, 1379. DOI: 10.1039/C1SC00069A.

- (15) Jagtap, S. A.; Bhanage, B. M. Semi-hydrogenation of alkynes using Ru/TPPTS as a biphasic recyclable catalyst in ethylene glycol-toluene solvent system. *Mol. Catal.* **2018**, *460*, 1-63. DOI: 10.1016/j.mcat.2018.09.008.
- (16) Moran, M. J.; Martina, K.; Bieliunas, V.; Baricco, F.; Tagliapietra, S.; Berlier, G.; Borggraeve, W. M. D.; Cravotto, G. Copper (0) nanoparticle catalyzed Z-Selective Transfer Semihydrogenation of Internal Alkynes. *Adv. Synth. Catal.* **2021**, *363*, 2850-2860. DOI: 10.1002/adsc.202100126.
- (17) Garbe, M.; Budweg, S.; Papa, V.; Wei, Z.; Hornke, H.; Bachmann, S.; Scalone, M.; Spannenberg, A.; Jiao, H.; Junge, K.; Beller, M. Chemoselective Semihydrogenation of Alkynes catalyzed by Manganese(I)-PNP Pincer Complexes. *Catal. Sci. Technol.* **2020**, *10*, 3994-4001. DOI: 10.1039/D0CY00992J.
- (18) Yoshii, T.; Umemoto, D.; Kuwahara, Y.; Mori, K.; Yamashita, H. Engineering of Surface Environment of Pd Nanoparticle Catalysts on Carbon Support with Pyrene-Thiol Ligands for Semihydrogenation of Alkynes. *ACS Appl. Mater. Interfaces* **2019**, *11*, 37708-37719. DOI: 10.1021/acsami.9b12470.
- (19) Mitsudome, T.; Urayama, T.; Yamazaki, K.; Maehara, Y.; Yamasaki, J.; Gohara, K.; Maeno, Z.; Mizugaki, T.; Jitsukawa, K.; Kaneda, K. Design of Core-Pd/Shell-Ag Nanocomposite Catalyst for Selective Semihydrogenation of Alkynes. *ACS Catal.* **2016**, *6*, 666-670. DOI: 10.1021/acscatal.5b02518.
- (20) Wu, C.; Chen, Y.; Shen, R.; Zhu, W.; Gong, Y.; Gu, L.; Peng, Q.; Guo, H.; He, W. The Promoting Effect of Low-Level Sulfidation in PdCuS Nanoparticles Catalyzed Alkyne Semihydrogenation. *Nano Research* **2018**, *11*, 4883-4889. DOI: 10.1007/s12274-018-2077-x.
- (21) Kaeffer, N.; Liu, H.-J.; Lo, H.-K.; Fedorov, A.; Copéret, C. An N-Heterocyclic Carbene Ligand Promotes Highly Selective Alkyne Semihydrogenation with Copper Nanoparticles Supported on Passivated Silica. *Chem. Sci.* **2018**, *9*, 5366-5371. DOI: 10.1039/C8SC01924J.